

## Novel Low-Temperature Behavior in Classical Many-Particle Systems

Robert D. Batten,<sup>1</sup> Frank H. Stillinger,<sup>2</sup> and Salvatore Torquato<sup>2,3,\*</sup>

<sup>1</sup>*Department of Chemical Engineering, Princeton University, Princeton, New Jersey 08544, USA*

<sup>2</sup>*Department of Chemistry, Princeton University, Princeton, New Jersey 08544, USA*

<sup>3</sup>*Princeton Materials Institute, Program in Applied and Computational Mathematics, Princeton Center for Theoretical Science, Princeton University, Princeton, New Jersey, 08544, USA;*

*School of Natural Sciences, Institute for Advanced Study, Princeton, New Jersey, 08544 USA*

(Received 25 May 2009; revised manuscript received 25 June 2009; published 30 July 2009)

We show that classical many-particle systems interacting with certain soft pair interactions in two dimensions exhibit novel low-temperature behaviors. Ground states span from disordered to crystalline. At some densities, a large fraction of normal-mode frequencies vanish. Lattice ground-state configurations have more vanishing frequencies than disordered ground states at the same density and exhibit vanishing shear moduli. For the melting transition from a crystal, the thermal expansion coefficient is negative. These unusual results are attributed to the topography of the energy landscape.

DOI: 10.1103/PhysRevLett.103.050602

PACS numbers: 05.20.-y, 61.50.Ah, 82.35.Jk, 82.70.Dd

Simple soft pair interactions are often used to model colloids, microemulsions, and polymers [1,2] and are capable of producing fascinating physical phenomena [3–10]. In this Letter, we show that single-component systems interacting via the “ $k$ -space overlap potential” produce unconventional physical properties, including classical disordered ground states, vanishing normal-mode frequencies, and negative thermal expansion. These results are attributed to the nature of the energy landscape for which we provide a descriptive picture.

We examine pairwise additive potentials  $v(r)$  that are bounded and absolutely integrable such that the Fourier transforms  $V(k)$  exist [9]. For a system of  $N$  identical particles within a volume  $\Omega$  with positions  $\mathbf{r}_i$  that interact via  $v(r)$  under periodic boundary conditions, the potential energy per particle is represented by

$$\phi = \frac{1}{2\Omega} \sum_{\mathbf{k}} V(\mathbf{k}) [|\rho(\mathbf{k})|^2 / N - 1], \quad (1)$$

where  $\rho(\mathbf{k}) = \sum_{j=1,N} \exp(i\mathbf{k} \cdot \mathbf{r}_j)$  are the Fourier coefficients of the density field.

We focus on the “ $k$ -space overlap potential,” which is the Fourier-space analog of the real-space “overlap” potential [11]. In two dimensions,  $V(k)$  is proportional to the intersection area between two disks of diameter  $K$  with centers separated by  $k$ ,

$$V(k) = \frac{2V_0}{\pi} \left[ \cos^{-1} \left( \frac{k}{K} \right) - \frac{k}{K} \left( 1 - \frac{k^2}{K^2} \right)^{1/2} \right], \quad (2)$$

for  $k \leq K$  and zero otherwise. This falls into the special class of pair potential functions in which  $V(k)$  is nonnegative and has compact support at some finite  $K$  [9]. We have previously constructed ground states for these  $V(k)$  in one, two, and three spatial dimensions [12–15]. At a specific density in each dimension, the integer, triangular, and body-centered cubic lattices are the unique ground states

[16]. Above these densities, other structures, periodic and disordered, are energy-degenerate ground states. In one dimension, these  $V(k)$  have an infinite number of “phase transitions” since ground states switch between Bravais and non-Bravais lattices with increasing density [9].

Given the unusual nature of the ground states, we seek to characterize additional ground-state and excited-state ( $T > 0$ ) properties for these  $V(k)$ . The overlap potential is our chosen model as it provides analytical expressions for  $V(k)$  and  $v(r)$  in two dimensions and is sufficiently short ranged for simulation. In the infinite-volume limit, the real-space pair potential function has the form

$$v(r) = \frac{V_0}{\pi r^2} \left[ J_1 \left( \frac{Kr}{2} \right) \right]^2, \quad (3)$$

where  $J_1$  is the Bessel function. It is bounded at  $r = 0$  and behaves as  $\cos^2(Kr/2 - 3\pi/4)/r^3$  for large  $r$ .

Since  $V(k)$  is positive and the minimum value of  $|\rho(\mathbf{k})|^2$  is zero, it is clear that any configuration in which the  $|\rho(\mathbf{k})|$ 's are constrained to their minimal value for  $0 < |\mathbf{k}| \leq K$  is a ground state [12–15]. We use the dimensionless parameter  $\chi = M(K)/dN$  as the fraction of degrees of freedom that are constrained, where  $M(K)$  is the number of independent wave vectors for  $0 < |\mathbf{k}| \leq K$  and  $dN$  is the total degrees of freedom for spatial dimension  $d$  [13]. With  $K = 1$  to fix the length scale of the system,  $\chi$  has an inverse relation to the number density  $\rho$ . As  $\chi$  goes to zero,  $\rho$  approaches infinity. For certain results,  $\chi$  is a more natural description of the system. Henceforth, we take  $V_0 = 1$  and assign particles a unit mass.

In previous work, it was reported that, in two dimensions, three classes of ground-state structures exist—disordered, wavy crystalline, and crystalline [13]—for the more general compact-support potentials. Disordered ground states are those in which constraining  $|\rho(\mathbf{k})|$  to be minimal for  $0 < |\mathbf{k}| \leq K$  does not implicitly minimize  $|\rho(\mathbf{k})|$  for  $|\mathbf{k}| > K$ . These are ground states for

$\chi < 0.58$  ( $\rho > 0.0346$ ). Wavy-crystalline ground states  $0.58 \leq \chi < 0.78$  ( $0.0253 < \rho \leq 0.0346$ ) are those in which constraining  $|\rho(\mathbf{k})|$  to be minimal for all  $0 < |\mathbf{k}| \leq K$  implicitly constrains some  $|\rho(\mathbf{k})|$  for  $|\mathbf{k}| > K$ . We have identified these as nonuniformly sheared triangular or square lattices. Last, the crystalline region is  $0.78 \leq \chi \leq 0.91 = \chi^*$  ( $\rho^* = 0.0219 \leq \rho \leq 0.0253$ ) where the lower bound  $\rho^*$  is the unique ground state [16]. Because of a dominance of relative minima and shape of the energy landscape at these densities, only the triangular lattice remains as a viable global minimum when numerically minimizing the potential energy [13]. However, at  $\chi = 0.78$ , the family of rhombical Bravais lattices are ground-state structures, and only at the upper limit,  $\chi = 0.91$ , is the triangular lattice the unique ground state. For crystalline structures, all  $|\rho(\mathbf{k})|$  are minimized except those associated with Bragg scattering. For  $\chi > 0.91$ , the ground states are not known, since the  $|\rho(\mathbf{k})|$ 's cannot be minimized for wave numbers equal to or greater than the location of the first Bragg peak of the triangular lattice. A more detailed explanation is provided in Ref. [17].

At  $T = 0$ , we investigated macroscopic properties for the family of rhombical Bravais lattices at  $\rho \geq \rho^*$  and find that for  $\rho = \rho^*$ , the triangular lattice has the lowest potential energy. Other Bravais lattices become energetically degenerate with the triangular lattice when the density is increased above  $\rho^*$ . This occurs as a sequence of events, and by  $\rho = 0.0253$  ( $\chi = 0.78$ ), all rhombical Bravais lattices have identical energies and pressures. Despite the use of a continuous potential, the pressure-density curve at  $T = 0$  for each rhombical Bravais lattice has a cusp. For the triangular lattice, this occurs at  $\rho^*$ , while for other lattices, the cusp occurs for some  $\rho > \rho^*$ . Correspondingly, for the triangular lattice, the isothermal compressibility vanishes when approaching  $\rho^*$  from below and is positive for all  $\rho > \rho^*$ . The shear modulus vanishes for the rhombical Bravais lattices since the system lacks restoring forces. As a consequence, the Poisson's ratio goes identically to unity for all  $\rho > \rho^*$ . These novel properties are a result of the ground states' insensitivity to the potential on these length scales, as previously suggested [16].

In the harmonic regime, we calculated the fraction of nonvanishing normal-mode frequencies to quantify the relative mechanical stability of ground states for  $\chi \leq 0.91$ . The eigenvalues of the Hessian correspond to the squared frequencies and the eigenvectors correspond to the directions of the normal modes. Modes with a vanishing frequency reveal a direction in the energy landscape in which the test configuration can be perturbed without an energy penalty. Along this direction, the energy landscape is flat, since there is a channel of depth equal to the global minimum running through the point associated with the test configuration. When all modes (excepting overall translation) have real frequencies, then all directions in the energy landscape are uphill.

With the overlap potential, the fraction of nonvanishing mode frequencies has a direct relation to  $\chi$ , shown in

Fig. 1. Since the fraction of modes with nonvanishing frequencies is indicative of the relative number of constrained degrees of freedom, one might expect a one-to-one relation between this fraction and  $\chi$ . However, for  $\chi < 0.5$ , each additional constrained  $\mathbf{k}$  yields two nonzero frequencies since the constraint on each  $\rho(\mathbf{k})$  implies  $\sum_{i=1,N} \sin(\mathbf{k} \cdot \mathbf{r}_i) = \sum_{i=1,N} \cos(\mathbf{k} \cdot \mathbf{r}_i) = 0$ . These constraints are apparently independent for  $\chi < 0.5$ .

For  $0.5 \leq \chi < 0.78$ , which includes some disordered and all wavy-crystalline ground states, nearly all of the frequencies are nonzero. Several representative configurations were used for the calculations in Fig. 1 and 92% to 98% of the frequencies were nonvanishing. In contrast, Bravais lattice ground states, which are energetically degenerate with amorphous ground states, have up to 12% fewer nonvanishing frequencies when equivalently constrained for  $\chi > 0.30$ . For the triangular lattice at  $\chi = 0.91$ , only two modes, those associated with overall translation, have vanishing frequencies (i.e., it is mechanically rigid). By reducing  $\chi$ , or increasing  $\rho$ , many modes become infinitely soft and have vanishing frequencies. The square lattice, a ground state for  $\chi \leq 0.78$ , is never mechanically stable, since a significant fraction of the normal modes have vanishing frequencies.

Using constant- $NVT$  molecular dynamics simulations with systems containing up to 780 particles, we estimated the fraction of nonzero frequencies via the excess heat capacity. Modes with vanishing frequencies do not actively contribute to the excess heat capacity in the harmonic approximation that is valid at low  $T$ . By equipartition, the fraction of nonvanishing mode frequencies is equal to the slope of the  $\phi$ - $T$  curve. For each  $\chi$ , a series of long molecular dynamics trajectories, initialized as the triangular lattice, was used to obtain equilibrium properties. For  $\chi < 0.5$ , the excess heat capacity was approximately  $2\chi$ , in agreement with the diagonalization of the Hessian. However, for all  $\chi \geq 0.5$ , the excess heat capacity was

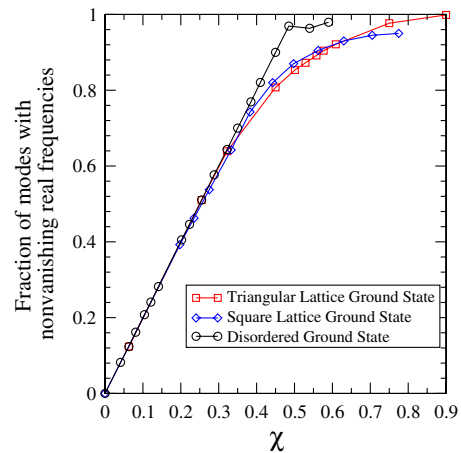


FIG. 1 (color online). Fraction of normal modes with nonvanishing, real frequencies as a function of  $\chi$  for disordered and crystalline structures for  $N = 780$ . The slope in the linear part is exactly two.

approximately unity, despite the use of the triangular lattice as the initial condition. This suggests that particles drift away from their initial lattice sites since there are insufficient restoring forces to maintain oscillations about them.

Figure 2 shows the density equation of state for several constant- $NPT$  simulations. Lower pressures were not considered because  $\chi$  would exceed 0.91 at  $T = 0$ . Upon heating at fixed pressure  $p$ , the system achieves a density maximum for all  $p \geq 1.7 \times 10^{-4}$  due to negative thermal expansion (NTE), an unusual behavior for single-component systems with isotropic interactions. Correspondingly, at constant  $\rho$ , with  $\rho \geq \rho^*$ , systems achieve a pressure minimum.

The mechanism for NTE shares some characteristics with that of the Gaussian core model (GCM) [3]. Configurations occurring at higher temperatures have a smaller increase in  $\phi$  upon compression than do configurations occurring at lower temperatures due to the shape of the energy landscape. However, this landscape-mediated mechanism for NTE with the  $k$ -space overlap potential contrasts with other well-known mechanisms. With this potential, NTE occurs with a single component via long-ranged attractive and repulsive forces, for both crystalline and amorphous structures. The GCM has only short-ranged repulsion. NTE behavior in substances like water or multicomponent solids requires anisotropic bonding so that the crystal structure collapses upon melting. In another mechanism, steep repulsions were tuned to coerce a crystal to densify upon heating [18], but the overlap potential is soft and NTE occurs for crystal and amorphous structures.

The overlap potential also produces unusual structural characteristics for positive  $T$ . Despite an effective soft core for small  $r$ , the interaction does not allow for increased local ordering upon isothermal compression. Isothermal compression results in a reduction in height of neighbor

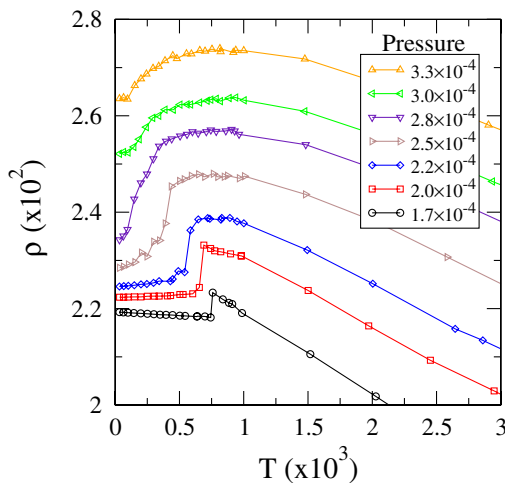


FIG. 2 (color online). Density as a function of temperature for several fixed pressures for 418 particles initialized as a triangular lattice and slowly heated. For  $p > 1.7 \times 10^{-4}$ , the systems show negative thermal expansion in the small  $T$  region.

peaks in the radial distribution function. The transition from crystal to liquid state is apparently continuous for most densities  $\rho > \rho^*$  since there is a lack of sharp discontinuities in the density shown in Fig. 2. Particles tend to flow away from the lattice sites instead of oscillating about them. Upon cooling, the local attractive forces are not strong enough to induce a local nucleation structure. The system instead remains amorphous while it continuously transitions to the appropriate ground state. Figure 3 shows two representative configurations for a system at  $\chi = 0.70$ . The left image is taken after allowing the triangular lattice to equilibrate at a temperature in the harmonic region (linear part of  $\phi$ - $T$  curve). Clearly particles do not oscillate about their initial lattice point as is typical for harmonic behavior. The right image is representative of the liquid state. We find that these results hold for various system sizes and shapes, including allowing for shape variation of the simulation cell.

These unusual properties are a result of the topography of the  $dN$ -dimensional potential energy landscape. Using these results and our experience with identifying ground states for these  $V(k)$  [12–15], we have constructed a schematic of a projection of the energy landscape for  $\chi \geq 0.5$  illustrated in Fig. 4. The center circle represents the triangular lattice point, the dark lines running through the center circle represent ground-state manifolds, and the crosses represent local minima located higher up in the landscape.

Configurations in the landscape, marked by diamonds, can fall by steepest decent trajectories (minimizing  $\phi$ ) to three possible outcomes—the triangular lattice point, a point on the ground-state manifold, or a local minimum. At a density of  $\rho^*$  ( $\chi = 0.91$ ), the landscape is devoid of ground-state manifolds. The only global minima in the energy landscape are associated with the triangular lattice, and from these points, every direction is uphill since all normal modes have nonzero frequencies (aside from overall translation). Upon compressing from  $\rho^*$ , the system enters the crystalline regime ( $0.78 \leq \chi < 0.91$ ) and more global minima appear as channels running through the triangular lattice point. These are the directions associated with vanishing normal-mode frequencies since there is no restoring force when moving along the manifold. Nearly

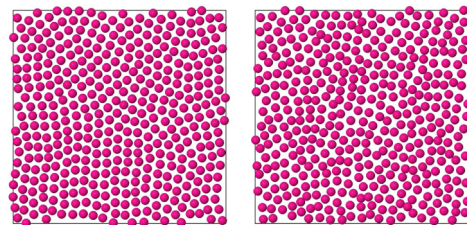


FIG. 3 (color online). Configurations at  $\rho = 2.86 \times 10^{-2}$ . (left) Harmonic region  $T = 10^{-4}$ ,  $p = 3.86 \times 10^{-4}$  and (right) liquid state  $T = 4 \times 10^{-4}$ ,  $p = 3.73 \times 10^{-4}$ . There is a lack of local nucleation and the transition from crystal to disorder is continuous. Particle sizes are chosen for clarity and are not reflective of the soft-core diameter.



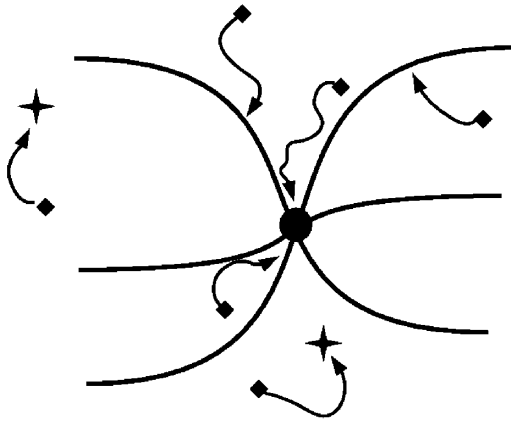


FIG. 4. Schematic of the ground-state manifolds (dark lines) in the energy landscape for  $\chi \geq 0.5$ . When minimizing the potential energy, initial configurations (diamonds) can fall by steepest descent trajectories to the triangular lattice (center point), amorphous ground states (dark lines), or to local energy minima (crosses). The conditions for each trajectory are described in the text.

all random initial conditions in this  $\chi$  range fall by steepest descent to local minima. Only those configurations immediately local to the lattice point (i.e., those that have been randomly perturbed from the lattice by less than 5% of the lattice spacing) return to the triangular lattice. Despite the existence of other ground-state configurations, the capture basins for these are too small to encounter by random searches.

Further compression into the wavy-crystalline region ( $0.58 \leq \chi < 0.78$ ) brings about a greater number of ground-state manifolds through the lattice point. Here, steepest descent trajectories from random configurations usually yield local minima and occasionally find wavy-crystalline ground states. Only infinitesimal random perturbations from the triangular lattice return to the lattice point. Larger perturbations yield wavy-crystalline structures on the manifold. In the disordered regime ( $\chi < 0.58$ ), the number of ground-state manifolds increases dramatically. In particular, for  $\chi < 0.5$ , even disordered ground states have vanishing frequencies. At each point along a manifold, there are several directions that provide no restoring force. This phenomenon is not portrayed in the two-dimensional schematic of a  $2N$ -dimensional hypersurface of Fig. 4. For  $\chi < 0.5$ , every initial condition we have tested results in a ground state. The energy landscape is evidently devoid of local minima.

In summary, we have ascertained several novel properties of a soft-matter system. Polymers or colloids may provide a realization of a system in which this potential serves as an appropriate effective interaction. With a single parameter  $\chi$ , or density, the relative mechanical stability can be controlled as mode frequencies “turn off” with increasing density. With attractive and repulsive forces in a single-component system, we have found a novel NTE

mechanism that applies for both crystalline and amorphous systems.

Because of the lack of an internal restoring force at low temperatures, these systems may show unusual transport properties. It is not currently known how such a potential affects dynamic properties such as self-diffusion and shear viscosity. Additionally, future work will look at the glassy behavior of such systems. With this potential, it may be possible that a glassy configuration exists in which no normal modes have vanishing nonzero frequencies (excepting translation) even though the ground-state crystal at the same density has some vanishing frequencies. This leads to a paradox in which the glassy state is subject to internal restoring forces but the ground state is not, which would require further exploration.

S. T. thanks the Institute for Advanced Study for its hospitality during his stay there. This work was supported by the Office of Basic Energy Sciences, U.S. Department of Energy, Grant No. DE-FG02-04-ER46108 and the National Science Foundation MRSEC Program (No. DMR-0820341).

\*Corresponding author.

torquato@electron.princeton.edu

- [1] P. J. Flory and W. R. Krigbaum, *J. Chem. Phys.* **18**, 1086 (1950).
- [2] C. N. Likos, *Phys. Rep.* **348**, 267 (2001).
- [3] F. H. Stillinger and D. K. Stillinger, *Physica (Amsterdam)* **244A**, 358 (1997).
- [4] F. H. Stillinger, *J. Chem. Phys.* **65**, 3968 (1976).
- [5] F. H. Stillinger and T. A. Weber, *J. Chem. Phys.* **70**, 4879 (1979).
- [6] R. D. Groot and P. B. Warren, *J. Chem. Phys.* **107**, 4423 (1997).
- [7] M. A. Glaser, G. M. Grason, R. D. Kamien, A. A. Kosmrlj, C. D. Santangelo, and P. Zihlerl, *Europhys. Lett.* **78**, 46004 (2007).
- [8] H. Cohn and A. Kumar, *Phys. Rev. E* **78**, 061113 (2008).
- [9] S. Torquato and F. H. Stillinger, *Phys. Rev. Lett.* **100**, 020602 (2008).
- [10] S. Torquato, *Soft Matter* **5**, 1157 (2009).
- [11] S. Torquato and F. H. Stillinger, *Phys. Rev. E* **68**, 041113 (2003). The real-space “overlap” potential arises in connection with local density fluctuations in point patterns.
- [12] Y. Fan, J. K. Percus, D. K. Stillinger, and F. H. Stillinger, *Phys. Rev. A* **44**, 2394 (1991).
- [13] O. U. Uche, F. H. Stillinger, and S. Torquato, *Phys. Rev. E* **70**, 046122 (2004).
- [14] O. U. Uche, S. Torquato, and F. H. Stillinger, *Phys. Rev. E* **74**, 031104 (2006).
- [15] R. D. Batten, F. H. Stillinger, and S. Torquato, *J. Appl. Phys.* **104**, 033504 (2008).
- [16] A. Sütő, *Phys. Rev. Lett.* **95**, 265501 (2005); *Phys. Rev. B* **74**, 104117 (2006).
- [17] R. D. Batten, F. H. Stillinger, and S. Torquato (to be published).
- [18] M. C. Rechtsman, F. H. Stillinger, and S. Torquato, *J. Phys. Chem. A* **111**, 12816 (2007).